19th Australasian Fluid Mechanics Conference
Melbourne, Australia
8-11 December 2014

Direct Numerical Simulations of the Dispersion of Molecules in Isotropic Turbulence.

D. Buaria[1], P. K. Yeung[2,3] and B. L. Sawford[4]

[1]School of Aerospace Engineering
Georgia Institute of Technology, Atlanta, Georgia 30332, USA

[2]Schools of Aerospace Engineering and Mechanical Engineering
Georgia Institute of Technology, Atlanta, Georgia 30332, USA

[3]Department of Mechanical and Aerospace Engineering
Hong Kong University of Science and Technology, Clear Water Bay, Hong Kong

[4]Department of Mechanical and Aerospace Engineering
Monash University, Clayton, Victoria 3800, Australia

Abstract

We describe new results from Direct Numerical Simulations for the dispersion of molecules over a range of values of Schmidt number Sc (the ratio of the kinematic viscosity to the molecular diffusivity) at a Taylor scale Reynolds number of 140. Our focus is on the statistics of single independent molecules and pairs of molecules. We show that at small times our results for both single molecules and pairs agree with the exact theoretical results of Saffman describing the interaction of the molecular diffusion and the turbulence within the dissipation sub-range. For high Sc numbers (low diffusivity) our results for the relative dispersion of pairs of molecules in the dissipation sub-range show an exponential growth regime with a rate constant which can be connected to a value $\tilde{B}_\theta \approx 5$ for the Batchelor constant, a parameter of the scalar variance spectrum.

Introduction

Most experimental observations or numerical calculations of turbulent flow are made at fixed points $\boldsymbol{x}$ in space at time t at which the velocity and the concentration of an inert scalar are given by $\boldsymbol{u}(\boldsymbol{x},t)$ and $c(\boldsymbol{x},t)$ respectively.

On the other hand, it is possible to describe the flow in terms of the velocity and concentration (and other quantities of interest) at a point moving with the flow.This is known as a Lagrangian description of the flow [6]. The position of this point $\boldsymbol{x}^+(t;\boldsymbol{x}_0,t_0)$ is a function of time and of some initial point $\boldsymbol{x}_0$ and time t_0 at which it was identified or "labelled". Its velocity is the velocity of the fluid where it happens to be at time t,

$$d\boldsymbol{x}^+/dt = \boldsymbol{u}^+(t;\boldsymbol{x}_0,t_0) = \boldsymbol{u}(\boldsymbol{x}^+(t),t) \tag{1}$$

We will use the superscript (+) to denote Lagrangian quantities, and quantities after the semi-colon are independent parameters. We refer to a point moving in this way as a fluid particle.

It is useful to generalize this description to include the joint effect of the fluid velocity and molecular diffusion on the motion of the particle [7, 8, 9]

$$d\boldsymbol{x}^{+(B)} = \boldsymbol{u}(\boldsymbol{x}^{+(B)}(t),t)dt + \sqrt{2\kappa}d\boldsymbol{W}(t) \tag{2}$$

where $d\boldsymbol{W}$ is the vector incremental Wiener process [5], κ is the molecular diffusivity and the superscript (B) denotes a Brownian particle. Equation (2) is a stochastic differential equation that effectively describes the motion of a molecule through the flow. For a given realization ω of the flow the statistics of the displacement of the molecule, averaged over the molecular motion, are described by the displacement PDF $P^{(\omega)}(\boldsymbol{x},t|\boldsymbol{x}',t')$ which is just the probability density of finding a molecule at position $\boldsymbol{x}$ at time t given that it was at position $\boldsymbol{x}'$ at time t'. Pope [7] showed that the molecular displacement PDF is equivalent to the scalar concentration due to an instantaneous point source of unit strength. The extension to general source conditions follows simply by integrating over the source distribution. Then averaging over different realizations of the flow field gives exact Lagrangian results for the moments of the scalar field

$$\langle c(\boldsymbol{x},t)\rangle = \int_{-\infty}^{t}\int_V P(\boldsymbol{x},t|\boldsymbol{x}',t')\,S(\boldsymbol{x}',t')\,d\boldsymbol{x}'dt' \tag{3}$$

$$\left\langle c^2(\boldsymbol{x},t)\right\rangle = \int_{-\infty}^{t}\int_V P\left(\boldsymbol{x},t|\boldsymbol{x}'_1,t'_1,\boldsymbol{x}'_2,t'_2\right) S\left(\boldsymbol{x}'_1,t'_1\right) \times S\left(\boldsymbol{x}'_2,t'_2\right) d\boldsymbol{x}'_1 dt'_1 d\boldsymbol{x}'_2 dt'_2 \tag{4}$$

where $S(\boldsymbol{x},t)$ is the source distribution, $P(\boldsymbol{x},t|\boldsymbol{x}',t') = \langle P^{(\omega)}(\boldsymbol{x},t|\boldsymbol{x}',t')\rangle$ is the displacement PDF for a molecule averaged over both the molecular and fluid motions, $P(\boldsymbol{x},t|\boldsymbol{x}'_1,t'_1,\boldsymbol{x}'_2,t'_2) = \langle P^{(\omega)}(\boldsymbol{x},t|\boldsymbol{x}'_1,t'_1)P^{(\omega)}(\boldsymbol{x},t|\boldsymbol{x}'_2,t'_2)\rangle$ is the probability density of finding two particles at the same location $\boldsymbol{x}$ at time t given their specified earlier positions. In general the n^{th} order scalar concentration moments can be specified in terms of the joint displacement statistics of n molecules.

Here we present new results from Direct Numerical Simulations (DNS) for the displacement statistics of single independent molecules and pairs of molecules over a range of Schmidt numbers. We analyze our results in particular limiting regimes (for example at small times or on small scales) and compare them with known theoretical results. In Section II we describe the DNS methodology. We present results for the dispersion of single molecules in Section III, the relative dispersion of pairs of molecules in Section IV and our conclusions in Section V.

DNS Calculations

The flow studied in this paper is isotropic turbulence computed using a Fourier pseudo-spectral approach on a 3D periodic domain. To obtain Lagrangian information we obtain the fluid particle velocity according to equation (1), using cubic-spline interpolation based on Eulerian data at neighboring grid points. Particle positions are updated at every time step using the same second-order Runge Kutta (predictor-corrector) scheme as for the Eulerian velocity field. Molecules are tracked by adding a Brownian motion contribution (equation (2)) at the predictor stage of each time step. The Brownian contribution over a finite time step Δt, is approximated by $dW_i = \sqrt{\Delta t}\xi_i$ where ξ_i is a standardized Gaussian random variable. Both the Eulerian solution domain and the Lagrangian population of fluid particles

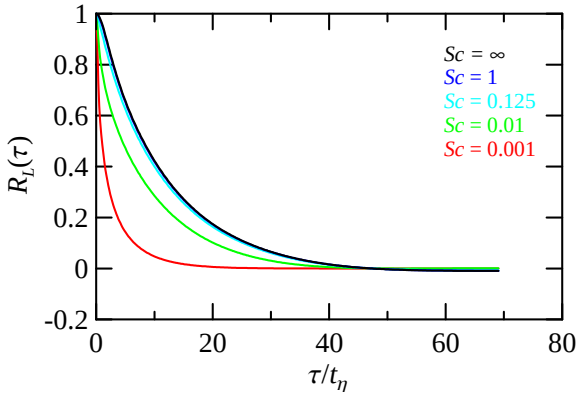

Figure 1: Lagrangian velocity correlation along molecular trajectories at $R_\lambda = 140$ for indicated values of Sc increasing from bottom to top.

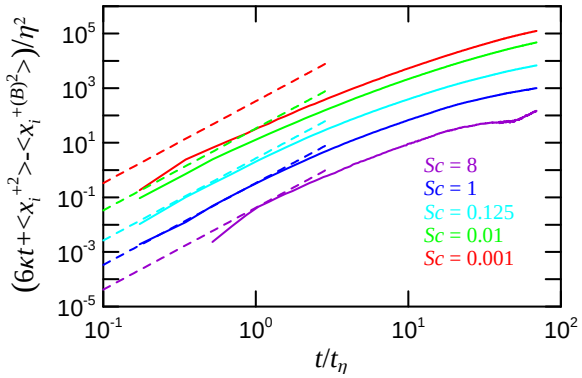

Figure 2: Minus the term representing the interaction between molecular and turbulent motions at $R_\lambda = 140$ for indicated values of Sc, increasing from top to bottom. The solid lines are DNS results and the dashed lines are Saffman's small-scale theory equation (9)

and molecules are divided uniformly across the memory of a large number of parallel processors.

In this paper we focus on DNS results for stationary isotropic turbulence at Taylor-scale Reynolds number $R_\lambda = 140$, which is just sufficiently high for the Eulerian energy spectrum to possess limited inertial range characteristics. The grid resolution is 256^3 and each grid spacing is equal to about two Kolmogorov length scales, $\eta = (\nu^3/\langle\epsilon\rangle)^{1/4}$, where $\langle\epsilon\rangle$ is the mean rate of dissipation of turbulence kinetic energy and ν is the kinematic viscosity. Statistical stationarity is maintained by a numerical scheme described in Donzis and Yeung [4]. Unlike Eulerian and scalar fields molecular path statistics are readily obtained at any Schmidt number without any special needs for temporal or spatial resolution. We have tracked molecules with Schmidt numbers from very low to very high: namely $Sc = 0.001$, 0.01, 0.125, 1, 8, 100 and 1000. To ensure adequate sampling we have tracked 4194304 fluid particles with random and uniformly distributed initial positions, with four molecules of each Sc being coincident with each fluid particle at time $t = 0$. This configuration gives us the capability to calculate the dispersion between fluid particles and molecules, as well as that between molecules which are initially coincident but move apart immediately due to the Brownian nature of molecular diffusion.

For a population of M fluid particles one can in principle form $M(M-1)/2$ pairs of these entities, with the initial separations being random but satisfying a continuous probability distribution. Thus, instead of specifying discrete values of initial separations (as in previous work), we use conditional sampling to obtain, say, results for particle pairs whose initial separations were in a finite range centered upon a certain value. Because the total number of particle pairs can become impractically large (approximately 8.8×10^{12} for $M = 4194304$), when we run a parallelized postprocessing code, we only count those pairs formed out of particles which are held by the same processor when processing the data.

Single Molecule Statistics

We consider first statistics of the fluid velocity along the trajectory of a molecule through the fluid. These statistics are of interest because they determine the mean concentration of a scalar field at finite Schmidt and Reynolds numbers. The most important quantity is the Lagrangian velocity correlation along the trajectory of a molecule

$$R_L^{(B)}(\tau) = \left\langle u_i^{+(B)}(t+\tau)u_i^{+(B)}(t)\right\rangle / \left\langle u_i^2\right\rangle \qquad (5)$$

where $\boldsymbol{u}^{+(B)} = \boldsymbol{u}(\boldsymbol{x}^{+(B)},t)$ is the Eulerian velocity at the location of the molecule at time t. $R_L^{(B)}$ is sometimes [8] referred to as the substance auto-correlation. Figure 1 shows the correlation as a function of the non-dimensional time lag τ/t_η, where the Kolmogorov time scale $t_\eta = (\nu/\langle\epsilon\rangle)^{1/2}$, for a range of Sc at $R_\lambda = 140$. The case $Sc = \infty$ corresponds to the motion of fluid particles in the absence of a molecular motion. We see that as the Schmidt number decreases and the influence of the molecular motions increases the correlation drops off more quickly with time, but strong departures from the fluid particle case are seen only for $Sc \ll 1$. The Lagrangian integral time scale

$$T_L^{(B)} = \int_0^\infty R_L^{(B)}(\tau)d\tau \qquad (6)$$

is an important measure of the rate of decay of the correlation. It is also an important quantity in practical terms since it determines the turbulent diffusivity $\frac{1}{3}\left\langle u_i^2\right\rangle T_L^{(B)}$ and so controls the rate of dispersion of scalar contaminants in the flow.

The velocity correlation is also important in practical terms since it determines the turbulent dispersion of the particles and hence the mean rate of spread, and consequent dilution, of a scalar contaminant. For molecular trajectories, the dispersion is given by

$$\left\langle x_i^{+(B)^2}(t)\right\rangle = 6\kappa t + 2\left\langle u_i^2\right\rangle \int_0^t \int_0^{t'} R_L^{(B)}(t'')dt''dt' \qquad (7)$$

Saffman [8] showed that the second term on the right hand side can be written as the sum of the dispersion of fluid particles $\left\langle x_i^{+2}\right\rangle$ plus a term Δ involving the interaction of the molecular and turbulent motions. Thus the interaction term is the residual after the direct molecular diffusion term and the fluid particle dispersion are subtracted from the molecular dispersion

$$\Delta = \left\langle x_i^{+(B)^2}\right\rangle - 6\kappa t + \left\langle x_i^{+2}\right\rangle \qquad (8)$$

On dissipation sub-range scales the flow field is smooth and Saffman used Taylor series expansions in both space and time to derive an exact result for the interaction term

$$\Delta/\eta^2 = -\tfrac{1}{3}Sc^{-1}(t/t_\eta)^3 + O(t^4), \qquad (9)$$

which is valid for $\left\langle x_i^{+(B)^2}(t)\right\rangle \ll \eta^2$ and $t \ll t_\eta$.

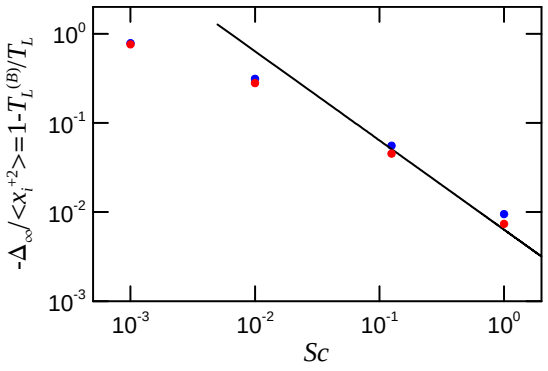

Figure 3: Minus the term representing the interaction between molecular and turbulent motions at large times $T \gg T_L^{(B)}$ as a function of Sc for $R_\lambda = 140$. The black symbols have been calculated directly from the dispersion estimates through equation (8) and the red symbols are calculated from estimates for the integral time scale. The solid line is Saffman's large-time theory equation (10).

We test Saffman's theory equation (9) in figure 2 where we plot $-\Delta/\eta^2$ calculated from equation (8) against t/t_η. For $Sc \geq 1/8$ the DNS results approach the theoretical limit for $t < t_\eta$, but with decreasing Sc the small-time behaviour of the DNS falls increasingly below the theory. This is because the direct molecular diffusion term $6\kappa t/\eta^2 > 1$ for $t/t_\eta > Sc$, which restricts the theory at these low Schmidt numbers to much smaller times than shown in figure 2 .

Saffman also derived an approximate theory for large times $t \gg T_L^{(B)}$ in which the interaction term is given by

$$\Delta_\infty \approx -a\sqrt{15} Sc^{-1} R_\lambda^{-1} \left\langle x_i^{+2} \right\rangle \qquad (10)$$

Using the large time limit $\left\langle x_i^{+(B)^2}(t) \right\rangle \approx 2\left\langle u_i^2 \right\rangle T_L^{(B)} t$ for the dispersion we can write this large-time interaction term as $\Delta_\infty / \left\langle x_i^{+2} \right\rangle = T_L^{(B)}/T_L - 1$.

Figure 3 shows the relative interaction term, calculated both directly from equation (8) at large times and indirectly from the Lagrangian integral time scales, as a function of Sc. The agreement between the two estimates is generally good, although it deteriorates with increasing Schmidt number as the interaction term gets smaller and more difficult to estimate. Saffman's theory is in reasonable agreement with the data at large Sc, but the predicted linear dependence on Sc inevitably breaks down at small Sc since $T_L^{(B)} \geq 0$. On a practical level, data like those presented in figure 3 are useful for modeling the dispersion of low-Sc scalars. For example, the integral time scale is an important parameter in Lagrangian stochastic models of dispersion, and to a first approximation, can simply be adjusted in dispersion models to allow for finite Sc effects.

Relative Dispersion of Pairs of Molecules

In this Section we present and analyze results for statistics of the separation of a pair of molecules. These statistics are important because they determine second-order concentration statistics of a scalar field, such as the scalar variance and the scalar dissipation rate, at finite values of the Schmidt number and Reynolds number.

As for the one-particle statistics discussed above, there are theoretical predictions under special limiting conditions which we can test against, and use to validate, our numerical results. For

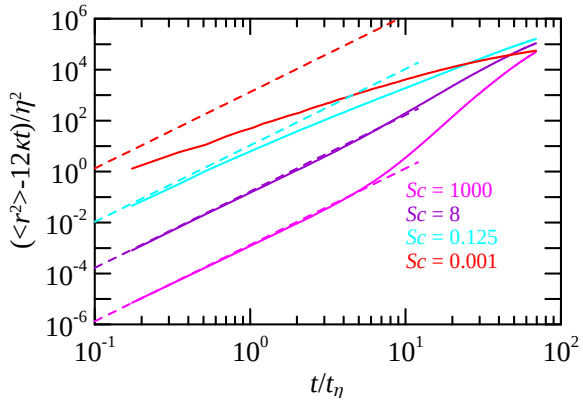

Figure 4: Relative dispersion of initially coincident molecule pair trajectories corrected for the direct molecular diffusion term at $R_\lambda = 140$ for indicated values of Sc, increasing from top to bottom. The solid lines are DNS results and the dashed lines are Saffman's small-scale theory equation (11).

example, in addition to the exact result for one-particle statistics on small-scales described above, Saffman [8] also derived the corresponding result for the relative dispersion of initially coincident pairs of molecules, which in non-dimensional form is

$$\left\langle r^2(t) \right\rangle / \eta^2 = 12 Sc^{-1} t/t_\eta + \frac{4}{3} Sc^{-1} (t/t_\eta)^3 + O(t^4) \qquad (11)$$

where $r(t)$ is the magnitude of the separation of a pair of molecules. Equation (11) holds for initially coincident molecules, $r_0 = r(0) = 0$ and for times such that $t \ll t_\eta$ and $\left\langle r^2(t) \right\rangle \ll \eta^2$. Figure 4 shows the mean-square separation of initially coincident pairs of molecules corrected for the direct effect of molecular diffusion as a function of time for various values of Schmidt number for $R_\lambda = 140$. For large Sc the DNS results agree almost exactly with the Saffman term representing the interaction of the turbulent and molecular motions for $t/t_\eta \lesssim 1$ and in fact are in good agreement for even larger times. With increasing Sc the Saffman term applies only up to increasingly shorter times because the direct molecular diffusion term becomes increasingly larger and drives the separation out of the influence of the dissipation range motions increasingly quickly.

Saffman's result is readily extended to particles with small initial separations $r_0 \ll \eta$

$$\left\langle r^2(t) \right\rangle / \eta^2 = (r_0/\eta)^2 + \tfrac{1}{3}(r_0/\eta)^2 (t/t_\eta)^2 + 12 Sc^{-1} t/t_\eta + \tfrac{4}{3} Sc^{-1} (t/t_\eta)^3 \qquad (12)$$

where the second term on the right, the so-called Batchelor term, is the leading order contribution from the turbulence and follows from a Taylor series expansion in time within the dissipation sub-range. The relative dispersion of a pair of molecules, corrected for both the direct molecular contribution and for the initial separation, is shown in figure 5 for $R_\lambda = 140$ and $Sc = 8$. We see that results over a range of initial separations, $r_0/\eta \leq 0.39$ collapse onto the Saffman term at small times. For larger initial separations, the Batchelor term dominates at the times shown. For $Sc = 1000$ (not shown here) this collapse to the Saffman term is limited to a smaller range of initial separations $r_0/\eta < 0.09$. In general, with decreasing Schmidt number (also not shown here), the collapse over initial separations extends to larger scales, although the interaction term eventually deviates from the Saffman form on the times shown here because the separation no longer remains within the dissipation sub-range.

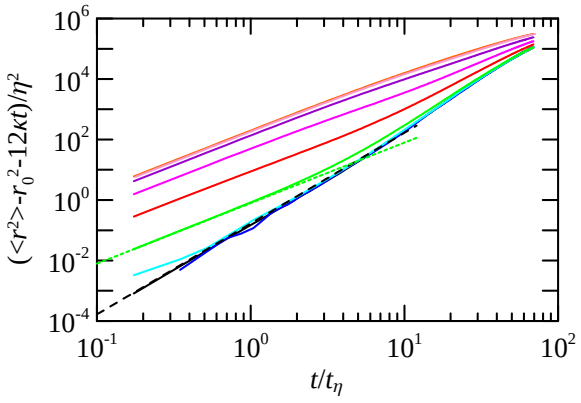

Figure 5: Relative dispersion of molecule pair trajectories, corrected for the direct molecular diffusion term and the initial separation, at $R_\lambda = 140$ for non-zero initial separations at $Sc = 8$. The solid lines are DNS results at (bottom to top) r_0/η = 0,0.09,0.39,1.5,6.2,25,97,350,580. The dashed line is Saffman's small-scale theory $4/3Sc^{-1}(t/t_\eta)^3$. The dotted line is the Batchelor term $1/3(r_0/\eta)^2(t/t_\eta)^2$ for $r_0/\eta = 1.5$.

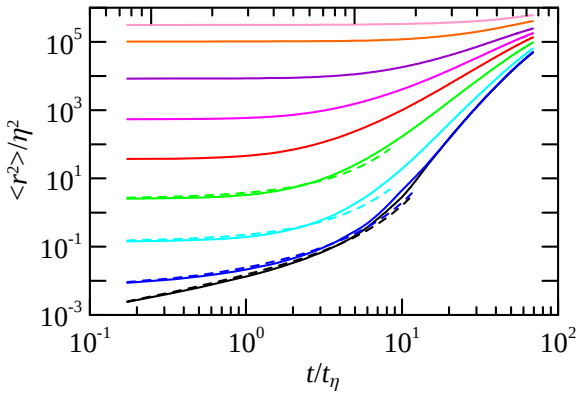

Figure 6: Relative dispersion of molecule pair trajectories at $R_\lambda = 140$ for non-zero initial separations at $Sc = 1000$. The solid lines are DNS results at (bottom to top) r_0/η = 0,0.09,0.39,1.5,6.2,25,97,350,580. The dashed lines are the large-Sc theory equation(13) with $\tilde{B}_\theta = 5$.

For large enough Schmidt numbers the separations remain with the dissipation sub-range for times much greater than the Kolmogorov time scale t_η. During this extended time period the separation process is subject to dissipation sub-range dynamics and an analytical solution for the growth is possible [1]. Within this regime we have

$$\left\langle r^2(t)\right\rangle/\eta^2 = (r_0/\eta)^2 \exp(2\tilde{B}_\theta^{-1} t/t_\eta) + 6Sc^{-1}\tilde{B}_\theta[\exp(2\tilde{B}_\theta^{-1} t/t_\eta) - 1] \qquad (13)$$

This exponential growth regime is controlled by the constant $\tilde{B}_\theta$ which has been identified [1] as the Batchelor constant which determines the viscous-convective regime of the scalar variance spectrum at large Sc.

In figure 6 we compare our DNS results for the mean square separation for $Sc = 1000$ and $R_\lambda = 140$ with equation (13). We see that for $r_0/\eta = 0$ the theory with $\tilde{B}_\theta = 5$ is a good fit to the data for times almost as large as $t/t_\eta = 10$. More generally the theory is a good fit to the data for $r_0/\eta \lesssim 1$ albeit over a decreasing time range with increasing initial separation. The value $\tilde{B}_\theta = 5$ for the Batchelor constant is consistent with previous estimates [1, 2, 3].

Conclusions

We have presented new DNS results for the dispersion of molecules over a range of Schmidt numbers at a Taylor scale Reynolds number of 140 in isotropic turbulence. Our results agree well with theoretical predictions on small space and time scales. From a fit of theory to our results at large Schmidt number we obtain an estimate $\tilde{B}_\theta = 5$ for Batchelor's constant which determines the viscous-convective regime of the scalar variance spectrum at large Sc. We expect that our results for the dependence of the Lagrangian integral timescale on the Schmidt number will be useful in Lagrangian modelling of turbulent dispersion at finite Schmidt and Reynolds numbers. Our future work will extend these results to higher Reynolds numbers where we will also be able to study the scaling behavior on larger scales, particularly within the Richardson range.

Acknowledgements

The authors gratefully acknowlegde support from the U.S. National Science Foundation, via Grant CBET-1235906. This work used the Extreme Science and Engineering Discovery Environment (XSEDE), which is supported by National Science Foundation grant number ACI-1053575. Computations leading to the results presented in this paper were performed on (primarily) Stampede at the Texas Advanced Computing Center as well as Kraken at the National Institute for Compuational Sciences at the University of Tennessee.

References

[1] Borgas, M. S., Sawford, B. L., Xu, S., Donzis, D. A. and Yeung, P. K., High schmidt number scalars in turbulence: Structure functions and lagrangian theory, *Phys. Fluids*, **16**, 2004, 3888–3899.

[2] Donzis, D. A., Sreenivasan, K. R. and Yeung, P. K., Scalar dissipation rate and dissipative anomaly in isotropic turbulence, *J. Fluid Mech.*, **532**, 2005, 199–216.

[3] Donzis, D. A., Sreenivasan, K. R. and Yeung, P. K., The Batchelor Spectrum for Mixing of Passive Scalars in Isotropic Turbulence, *Flow Turbul. Combust.*, **85**, 2010, 549 – 566.

[4] Donzis, D. A. and Yeung, P. K., Resolution effects and scaling in numerical simulations of passive scalar mixing in turbulence, *Physica D*, **239**, 2010, 1278 – 1287.

[5] Gardiner, C., *Handbook of Stochastic Methods for Physics, Chemistry and the Natural Sciences*, Springer, Berlin, 1983.

[6] Monin, A. S. and Yaglom, A. M., *Statistical Fluid Mechanics*, volume I, MIT Press, Cambridge, 1971.

[7] Pope, S. B., The vanishing effect of molecular diffusivity on turbulent dispersion: Implications for turbulent mixing and the scalar flux, *J. Fluid Mech.*, **359**, 1998, 299 – 312.

[8] Saffman, P. G., On the effect of the molecular diffusivity in turbulent diffusion, *J. Fluid Mech.*, **8**, 1960, 273–283.

[9] Sawford, B. L. and Hunt, J. C. R., Effects of turbulence structure, molecular diffusion and source size on scalar fluctuations in homogeneous turbulence, *J. Fluid Mech.*, **165**, 1980, 373 – 400.